Materials Science and Engineering A 528 (2011) 5259–5263

Contents lists available at ScienceDirect

Materials Science and Engineering A

journal homepage: www.elsevier.com/locate/msea

Evaluation of indentation tensile properties of Ti alloys by considering plastic constraint effect

Kug-Hwan Kim[a,*], Young-Cheon Kim[a], Eun-chae Jeon[b], Dongil Kwon[a]

[a] Department of Materials Science and Engineering, Seoul National University, Seoul 151-744, Republic of Korea
[b] Division of Nano-Mechanical Systems, Korea Institute of Machinery & Materials, Daejeon, 305-343, Republic of Korea

ARTICLE INFO

Article history:
Received 5 January 2011
Received in revised form 9 March 2011
Accepted 9 March 2011
Available online 17 March 2011

Keywords:
Spherical indentation test
Representation method
Ti alloys
Plastic constraint factor

ABSTRACT

The uniaxial tensile properties of metallic materials can be determined by representing the indentation stress and strain by the load/depth parameters from instrumented indentation tests using a spherical indenter. Here we propose a modified algorithm for evaluating the tensile properties of Ti alloys with low E/σ_y values by taking into account the plastic constraint effect in low-strain regions. The ratio of elastic modulus to yield strength, E/σ_y, can be interpreted as a measure of the amount of deformation plastically accommodated during indentation. For low E/σ_y materials, deformation is elastic-dominated, so less constraint occurs than in high E/σ_y materials. Finite element methods and spherical indentation tests were used to explore the constraint effect for a variety of materials characterized by different E/σ_y. The constraint factors were plotted as $(E/\sigma_y)(a/R)$ based on expanding cavity model. The modified approach was experimentally verified by comparing tensile properties from uniaxial tensile test and instrumented indentation tests.

1. Introduction

Indentation testing, originally developed to evaluate hardness, has been extended in recent decades to characterize other mechanical properties such as tensile properties [1–6], fracture toughness [7–9] and residual stress [10–12]. Although many indentation experiments are conducted with sharp indenter, e.g. the Vickers indenter at macro scales [13–16] and the Berkovich three-side pyramid indenter at nano scales [17,18], the spherical indenter has distinct advantages in evaluating diverse material properties.

The usual algorithm for obtaining uniaxial stress-strain curve and tensile properties by the spherical indentation test has four steps; step 1—determination of contact area, step 2—representation of true stress and strain, step 3—fitting to constitutive equation, and step 4—evaluation of tensile properties [19]. This method was registered as an ISO technical report in 2008, ISO/TR29381 [20]. The most important step is step 2, representation of stress and strain.

Following Meyer's approach [21], Tabor (1951) proposed that the indentation mean pressure (p_m) can be converted to stress in uniaxial testing, and d/D to strain [1]. In general, the amount of deformation or strain around the indentation will vary from point to point. However, Tabor suggested that when full plasticity is reached, there will exist average or mean value in the deformed zone. On the basis of experimental results, Tabor proposed the following relations:

$$\sigma_r = \frac{p_m}{\psi} \tag{1}$$

$$\varepsilon_r = f\left(\frac{d}{D}\right) \tag{2}$$

where σ_r, ε_r are the 'representative' stress and strain induced by indentation, and ψ is the plastic constraint factor. This relationship is widely used in indentation research and there are many definitions of the plastic constraint factor, ψ. For most metallic materials, a constant value of 3.0 is used by assuming a fully plastic indentation process [1,7,19,20,22–24,26].

However, it is difficult to use the above representation method directly for materials with low E/σ_y (<300) values such as Ti alloys, due to their low constraint effect in low-strain region. The constraint effect evolving during indentation is strongly dependent on the comparative amounts of elastic and plastic deformation as expressed by the ratio of elastic modulus to yield strength, E/σ_y. This parameter is the reciprocal of the elastic strain and can therefore be used as a measure of the plastically accommodated amount of deformation during indentation. Instead of E/σ_y, Johnson (1970) used $(E/\sigma_y)(a/R)$, which can be interpreted as the ratio of the strain imposed by the indenter to the elastic strain of the material [25]. Fig. 1 is a schematic representation of the relation between p_m/σ_r and $(E/\sigma_y)(a/R)$. Matthews (1980) calculated the pressure distribution beneath the indenter and correlated the indentation pressure

* Corresponding author. Tel.: +82 2 880 8404; fax: +82 2 886 4847.
E-mail address: samadhi0@snu.ac.kr (K.-H. Kim).

0921-5093/$ – see front matter © 2011 Elsevier B.V. All rights reserved.
doi:10.1016/j.msea.2011.03.052

Table 1
Chemical compositions (as received).

Material	C	Si	Mn	P	S	Cu	Ni	Cr	Mo	V	Al	Fe	Sn
SKD61	0.392	1.00	0.365	0.024	0.005	0.106	0.239	5.11	1.13				
SCM21	0.180	0.350	0.850	0.030	0.030			1.20	0.300				
S45C	0.440	0.259	0.750	0.014	0.004		0.010	0.020					
SK4	1.00	0.350	0.500	0.030	0.030								
SKS3	1.00	0.350	1.20	0.030	0.030	0.250	0.250	1.00					
Ti–5Al–2.5Sn	0.100										6.00	0.500	3.00
Ti–6Al–4V	0.100									4.50	6.75	0.400	
Ti–6Al–6V–2Sn	0.050									6.00	6.00	1.00	2.50
Ti–7Al–4Mo	0.100										6.80	0.300	

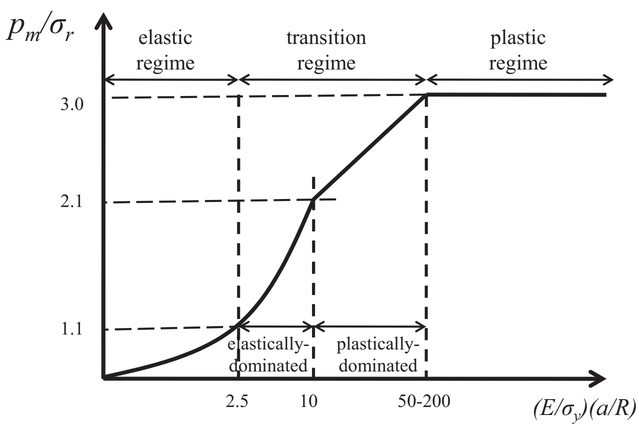

Fig. 1. A schematic representation of the relation between p_m/σ_r and $(E/\sigma_y)(a/R)$.

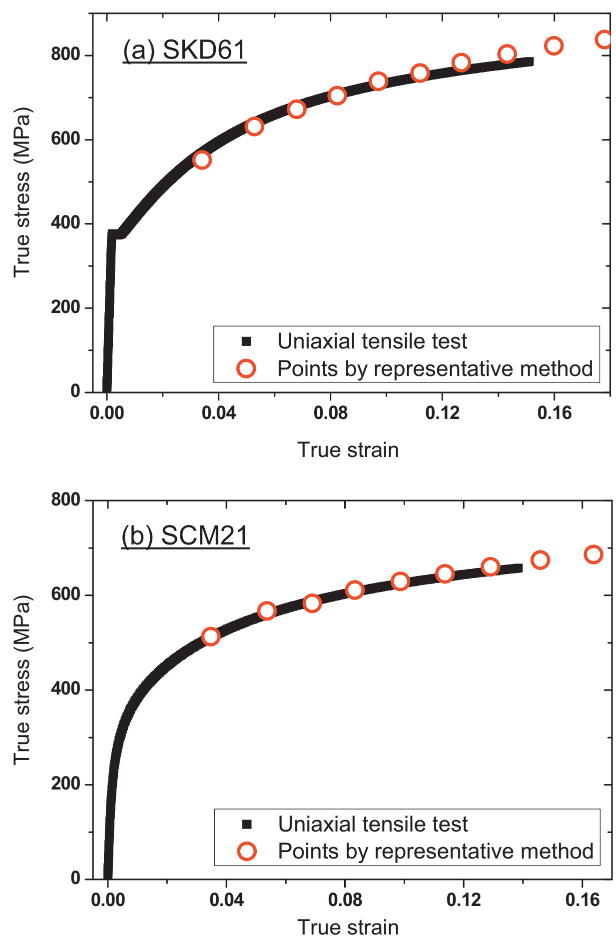

Fig. 2. The stress–strain curves evaluated by instrumented indentation testing for the carbon steels.

with the strain-hardening exponent [27]. Taljat et al. (1988) also the found that the plastic constraint factor decrease with increasing strain-hardening exponent [28]. Gao et al. (2006) developed analytical solutions for power-law and linear hardening materials [29]. Kumaraswamy et al. (2006, 2010) showed the temperature dependence of the constraint factor under elastic-plastic transition deformation conditions [30,31]. Lee et al. (2007) assessed the constraint factor using a relative depth for bulk metallic materials [32].

In this study, we propose a modified representation method for Ti alloys that takes into account their constraint effect in the low-strain region. Finite element methods and spherical indentation tests were performed to explore the constraint effect for a variety of materials characterized by different ratios of elastic modulus to yield strength, E/σ_y.

2. Experiments

Four Ti alloy samples were prepared for spherical indentation and uniaxial tensile testing, and five carbon steels were also examined for comparison. The chemical compositions of specimen were summarized in Table 1. Spherical indentation tests were conducted using the AIS2100 instrumented indentation system (Frontics, Inc., Korea) with force resolution 55 mN and displacement resolution 100 nm. The indenter was a tungsten carbide ball of radius 250 μm, and the final depth was 100 μm. The indentation speed was 0.3 mm/min and multiple unloadings down to 50% of maximum load at each point were applied. The specimen surface was mechanically ground using emery paper and finely polished with 0.5 μm alumina powder. Uniaxial tensile tests were performed using Instron 5582 (Instron, Inc., USA) at cross-head speed 0.5 mm/min for specimens with gauge length 25 mm and diameter 6 mm, according to the ASTM E-8M standard [33]. The elastic moduli of the samples were measured by an ultrasonic pulse-echo technique using a two-channel digital real-time oscilloscope on TDS220 (Tektronics, Inc., USA).

Finite element simulations were performed using the ABAQUS/Standard 6.5 code to determine the transition regime by evaluating the contact area during indentation loading. The indenter was considered as a rigid spherical ball. The specimen was modeled using the 2D axially symmetric isotropic element

Table 2
Material properties from uniaxial tensile tests and ultrasonic method.

Material	σ_y (MPa)	σ_{UTS} (MPa)	n	E (GPa)	ν
SKD61	371.45	781.33	0.241	213.55	0.302
SCM21	271.04	653.39	0.222	193.78	0.303
S45C	362.72	774.19	0.258	211.88	0.279
SK4	435.29	748.62	0.180	203.93	0.311
SKS3	434.95	755.50	0.218	209.61	0.310
Ti–5Al–2.5Sn	885.57	1038.01	0.066	130.31	0.294
Ti–6Al–4V	937.13	1099.82	0.080	109.64	0.333
Ti–6Al–6V–2Sn	1009.23	1172.56	0.076	121.78	0.324
Ti–7Al–4Mo	1030.57	1141.56	0.055	132.10	0.339

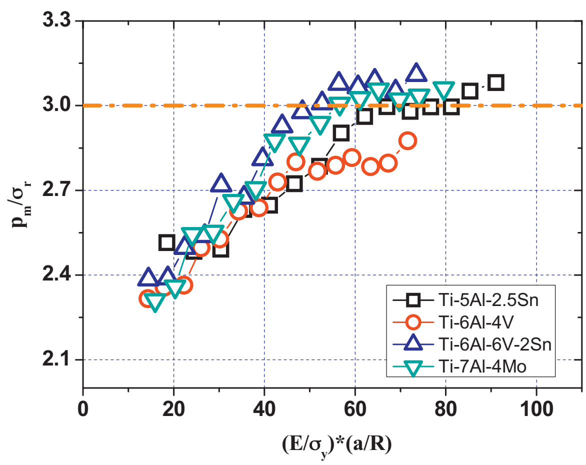

Fig. 3. A plastic constraint factor as a function of $(E/\sigma_y)(a/R)$ for Ti alloys.

(CAX4R) and the number of elements was approximately 40,000 by biased meshing. A 0.2 friction coefficient at the indenter-specimen interface was used in the computations. The input material properties were the tensile stress-strain curves, elastic modulus, and Poisson's ratio for each material listed in Table 2.

3. Results and discussion

3.1. Comparison of indentation and tensile test results

The stress-strain curves evaluated by the instrumented indentation test were compared with those evaluated by uniaxial tensile test (see Fig. 2). The ferrous metals showed good agreement with the uniaxial tensile test with a constant plastic constraint factor 3.0 throughout the strain region. In addition, the error range in yield strength and ultimate tensile strength obtained was ±10% of the tensile test results. However, the results for Ti alloys underestimated the stress at low strains, thus caused the underestimation of yield strength (see Fig. 4).

Table 3
$(E/\sigma_y)(a/R)$ with increasing a/R from finite element simulation for (a) SKD61 and (b) Ti–5Al–2.5Sn.

SKD61			Ti–5Al–2.5Sn		
Depth (μm)	a/R	$(E/\sigma_y)(a/R)$	Depth (μm)	a/R	$(E/\sigma_y)(a/R)$
1.56	0.0142	45.05	1.76	0.0140	11.30
2.66	0.0189	59.83	3.26	0.0200	16.12
3.98	0.0239	75.47	4.50	0.0238	19.20
6.07	0.0292	92.20	6.39	0.0292	23.53
8.48	0.0348	110.08	9.13	0.0349	28.15
14.12	0.0471	148.94	16.97	0.0491	39.64
19.81	0.0541	170.97	20.41	0.0544	43.88
32.36	0.0694	219.29	32.85	0.0697	56.28

Table 3 shows the development of $(E/\sigma_y)(a/R)$ with increasing a/R for SKD61 and Ti–5Al–2.5Sn from the finite element method. Note that increasing a/R corresponds to increasing penetration depth. The boundary between the transition and fully plastic regime is a little ambiguous, but Johnson suggested that fully plastic deformation is reached at a value of $(E/\sigma_y)(a/R) \approx 40$ [25]. The results show that the SKD61 with high E/σ_y value easily exceeds the value of $(E/\sigma_y)(a/R) \approx 40$, the boundary between transition and fully plastic regime, at very low depth, thus reaching the fully plastic regime. For materials with high E/σ_y (>300), such as ferritic and austenitic steels, the deformation easily moves to the fully plastic regime even at very small indentation strain, and it is thus appropri-

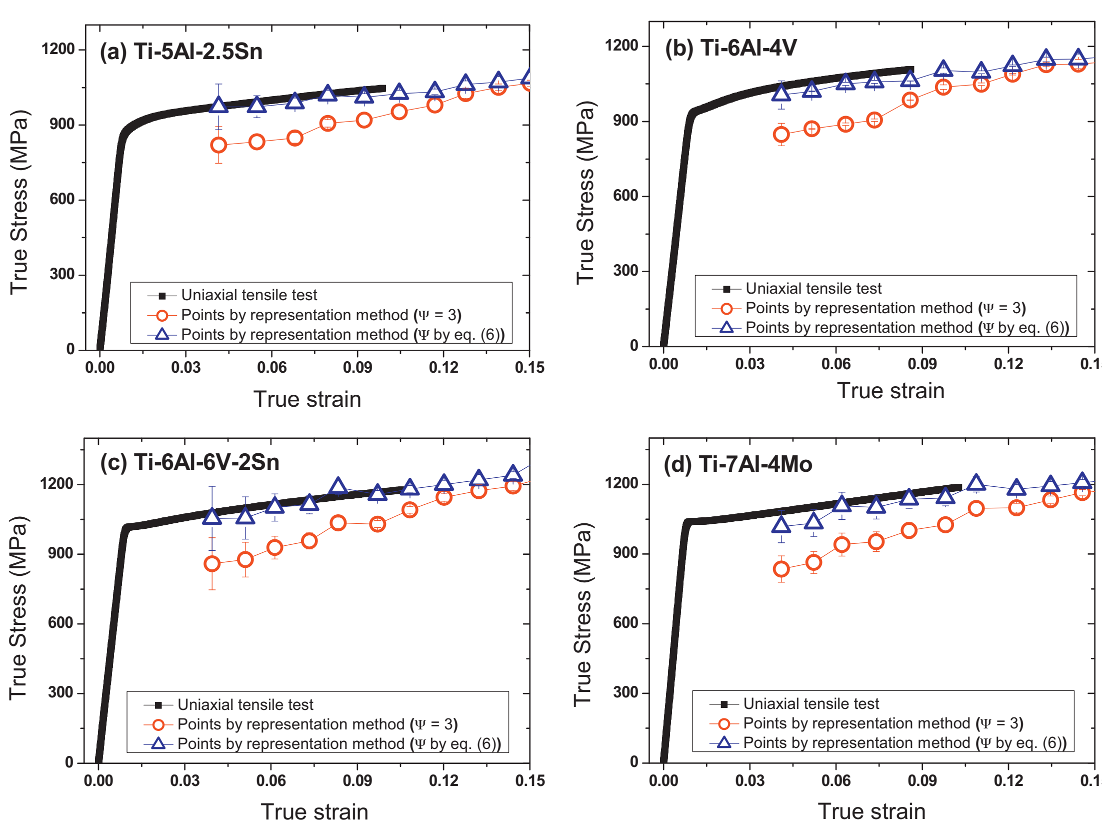

Fig. 4. Comparison of the tensile curves from tensile tests and instrumented indentation tests for the Ti alloys (a) Ti–5Al–2.5Sn, (b) Ti–6Al–4V, (c) Ti–6Al–6V–2Sn and (d) Ti–7Al–4Mo.

Table 4
Tensile properties from tensile tests and spherical indentation tests.

Material	Yield strength (MPa)			Ultimate tensile strength (MPa)		
	Tensile	Indentation	Error (%)	Tensile	Indentation	Error (%)
SKD61	371.45	370.02	−0.38	781.33	777.55	−0.48
SCM21	271.04	311.24	14.83	653.39	656.31	0.45
S45C	362.72	358.01	−1.30	774.19	761.48	−1.64
SK4	435.29	463.84	6.56	748.62	781.24	4.36
SKS3	434.95	476.74	9.61	755.50	805.90	6.67
Ti–5Al–2.5Sn	885.57	953.23	−7.64	1038.01	1064.89	2.59
Ti–6Al–4V	937.13	987.36	5.36	1099.82	1026.47	−6.67
Ti–6Al–6V–2Sn	1009.23	1070.28	6.05	1172.56	1205.11	2.78
Ti–7Al–4Mo	1030.57	1065.30	3.37	1141.56	1144.74	0.28

ate to use a constant constraint factor in defining the representative stress.

On the other hand, Ti–5Al–2.5Sn with low E/σ_y value cannot reach the boundary of the transition/fully plastic regime in the low penetration depth. The Ti alloys have a low elastic modulus (nearly 110 GPa) and high yield strength, so the deformation in elastic–plastic transition regime may be dominant. Eventually the constraint factor increases until the deformation reaches the fully plastic regime and the value is below 3.0.

3.2. Modification of plastic constraint factor

Because of the results above, the plastic constraint factor for Ti alloys at low strain was modified for accurate evaluation of tensile properties. The ratio of indentation pressure to uniaxial stress was correlated in a nondimensional function of $(E/\sigma_y)(a/R)$, which may be interpreted as the ratio of the representative strain imposed beneath the indenter (a/R) to the elastic strain (σ_y/E). Thus, a high $(E/\sigma_y)(a/R)$ value means that plastic deformation dominates elastic deformation:

$$\frac{a/R}{\sigma_y/E} \approx \frac{\kappa\varepsilon_r}{\varepsilon_y} \approx \frac{\kappa\varepsilon_p}{\varepsilon_y} \tag{3}$$

where κ is a experimental constant known as 5.0 by Tabor [1].

Fig. 3 shows the plastic constraint factor as a function of $(E/\sigma_y)(a/R)$ for the four Ti alloys. Johnson's expanding cavity model is often employed to describe stress responses of elastic–plastic materials because of its simplicity. However, the model has a critical limitation: the plastic hardening effect in metal was not considered. In this study, we adopted Gao's modified expanding cavity model [29] to find the relation between p_m/σ_r and $(E/\sigma_y)(a/R)$. Eq. (4) was obtained under the assumptions of isotropic hardening, power-law hardening and monotonic loading, and Hencky's deformation behavior:

$$\frac{p_m}{\sigma_y} = \frac{2}{3}\left\{\left(1-\frac{1}{n}\right)+\frac{1}{n}\left(\frac{1}{4}\frac{E}{\sigma_y}\frac{a}{R}\right)^{n}\right\} \tag{4}$$

This model reduces to Johnson's expanding cavity model for elastic-perfectly plastic materials when the strain-hardening effect is not considered $(n \to 0)$.

To define the plastic constraint factor, we correlated the indentation pressure with the flow stress rather than the yield stress. From the strain distribution beneath the indenter, the representative strain was defined as $0.25a/R$ [29]. By adopting the power-law hardening equation, we obtained the relation

$$\psi = \frac{p_m}{\sigma_r} = \frac{p_m}{K\varepsilon_r^n} = \frac{p_m}{\sigma_y}\left(\frac{1}{4}\frac{E}{\sigma_y}\frac{a}{R}\right)^{-n} = \frac{2}{3}\left\{\left(1-\frac{1}{n}\right)\left(\frac{1}{4}\frac{E}{\sigma_y}\frac{a}{R}\right)^{-n}+\frac{1}{n}\right\} \tag{5}$$

where K is the strength coefficient.

On the other hand, Eq. (5) predicts lower indentation pressure values than those experimentally measured due to assumption that core are purely hydrostatic. The best estimate of the indentation pressure for the spherical cavity model was proposed through adding $2\sigma_y/3$ to the indentation pressure based on Johnson [25], Feng et al. [34]. The final relation between p_m/σ_r and $(E/\sigma_y)(a/R)$ is:

$$\psi = \frac{p_m}{\sigma_r} = \frac{2}{3}\left\{\left(1-\frac{1}{n}\right)\left(\frac{1}{4}\frac{E}{\sigma_y}\frac{a}{R}\right)^{-n}+\left(1+\frac{1}{n}\right)\right\} \tag{6}$$

However, we need to predetermine the yield strength in order to evaluate the stress–strain curve using Eq. (6) by spherical indentation test only. Hoyt suggested that the material constant A in Meyer equation (Eq. (7)) is the measure of the resistance of metals to initial penetration [35].

$$\frac{P}{d^2} = A\left(\frac{d}{D}\right)^{m-2} \tag{7}$$

George et al. proposed an empirical relationship between the 0.2% offset yield strength and the constant A that can be written as [36]

$$\sigma_y = c \times A \tag{8}$$

where c is a constant that varies with the specific material class. George et al. found c to be 0.224 for the sheet steel grades. In this study, the c value for Ti alloys was determined with a known value of σ_y, the value was 0.3. The results for yield strength using Eq. (8), as listed in Table 4, show good agreement with those of the uniaxial tensile test.

3.3. Stress–strain curve calculation

Fig. 4 compares the stress–strain curves for Ti alloys obtained by the modified representation approach to tensile curves from uniaxial tensile testing, and Table 4 summarizes the tensile properties obtained from indentation and tensile test. The yield and tensile strengths from IIT were within ±10% of those from tensile tests.

4. Conclusion

A modified representation method was proposed to estimate indentation tensile properties for materials with low E/σ_y value, such as Ti alloys. For low E/σ_y materials, the elastic-dominated deformation occurred compared to high E/σ_y materials; this caused less constraint in the low-strain region during indentation. The constraint factors were plotted as $(E/\sigma_y)(a/R)$, i.e. the ratio of the strain imposed beneath the indenter to the elastic strain in the material, and a relation between the two parameters was proposed based on Gao's modified expanding cavity model. Tensile properties from the spherical indentation test were experimentally verified by comparison to the stress-strain curve and tensile properties from the uniaxial tensile test. The yield and tensile strength obtained were within ±10% of those from tensile tests.

Acknowledgements

This study was supported in part by the fundamental R&D program for the Core Technology of Materials (K0001337) funded by the Ministry of Knowledge Economy, Republic of Korea, and in part by the Converging Research Center Program (2010K001432) through the Ministry of Education, Science and Technology, Republic of Korea.

References

[1] D. Tabor, The Hardness of Metals, Clarendon Press, Oxford, 1951.
[2] B. Taljat, T. Zacharia, F. Kosel, Int. J. Solids Struct. 35 (1998) 4411.
[3] M. Dao, N. Chollacoop, K.J. Van Vliet, T.A. Venkatesh, S. Suresh, Acta Mater. 49 (2001) 3899.
[4] N. Chollacoop, M. Dao, S. Suresh, Acta Mater. 51 (2003) 3713.
[5] E.G. Herbert, G.M. Pharr, W.C. Oliver, B.N. Lucas, J.L. Hay, Thin Solid Films 398–399 (2001) 331.
[6] J.L. Bucaille, S. Stauss, E. Felder, J. Michler, Acta Mater. 51 (2003) 1663.
[7] J.S. Lee, J.I. Jang, B.W. Lee, Y. Choi, S.G. Lee, D. Kwon, Acta Mater. 54 (2006) 1101.
[8] B.R. Lawn, E.R. Fuller, J. Mater. Sci. 10 (1975) 2016.
[9] T.S. Byun, J.W. Kim, J.H. Hong, J. Nucl. Mater. 252 (1998) 187.
[10] S. Suresh, A.E. Giannakopoulos, Acta Mater. 465 (1998) 755.
[11] Y.H. Lee, D. Kwon, Acta Mater. 52 (2004) 1555.
[12] Y.H. Lee, J.Y. Kim, J.S. Lee, K.H. Kim, J.Y. Koo, D. Kwon, Philos. Mag 86 (2006) 5497.
[13] J.M. Antunes, A. Cavaleiro, L.F. Menezes, M.I. Simões, J.V. Fernandes, Surf. Coat. Techol. 149 (2002) 27.
[14] M. Mata, M. Anglada, J. Alcalá, J. Mater. Res. 17 (2002) 968.
[15] D. Nolan, V. Leskovsek, M. Jenko, Surf. Coat. Technol. 201 (2006) 182.
[16] M.M. Chaudhri, Acta Mater. 46 (1998) 3047.
[17] M.F. Doerner, W.D. Nix, J. Mater. Res. 1 (1986) 601.
[18] J.Y. Kim, S.K. Kang, J.R. Greer, D. Kwon, Acta Mater. 56 (2008) 3338.
[19] J.Y. Kim, K.W. Lee, J.S. Lee, D. Kwon, Surf. Coat. Technol. 201 (2006) 4278.
[20] ISO/TR29381, Metallic materials – measurement of mechanical properties by an instrumented indentation test – indentation tensile properties, ISO, 2008.
[21] E. Meyer, Phys. Z. 9 (1908) 66.
[22] J.H. Ahn, D. Kwon, J. Mater. Res. 16 (2001) 3170.
[23] S.H. Kim, B.W. Lee, Y. Choi, D. Kwon, Mater. Sci. Eng. A: Struct. 415 (2006) 59.
[24] K.W. Lee, K.H. Kim, J.Y. Kim, D. Kwon, J. Phys. D: Appl. Phys. 41 (2008) 074014.
[25] K.L. Johnson, Contact Mechanics, Cambridge University Press, Cambridge, 1985.
[26] A.C. Fischer-Cripps, Nanoindentation, Springer, New York, 2002.
[27] J.R. Matthews, Acta Metall. 28 (1980) 311.
[28] B. Taljat, T. Zacharia, F. Kosel, Int. J. Solids Struct. 35 (1980) 4411.
[29] X.-L. Gao, X.N. Jing, G. Subhash, Int. J. Solids Struct. 43 (2006) 2193.
[30] A. Kumaraswamy, B. Venkataraman, Scripta Mater. 54 (2006) 493.
[31] A. Kumaraswamy, V. Vasudeva Rao, Mater. Sci. Eng. A 527 (2010) 6230.
[32] Y.H. Lee, J.Y. Kim, U.-B. Baek, D. Kwon, J. Mater. Res. 22 (2007) 2895.
[33] ASTM E 8/E 8M, Standard Test Methods for Tension Testing of Metallic Materials, ASTM International, PA, 2002.
[34] G. Feng, S. Qu, Y. Huang, W.D. Nix, J. Mater. Res. 24 (2009) 704–718.
[35] S.L. Hoyt, Trans. Am. Soc. Steel Treat. 6 (1924) 396.
[36] R.A. George, S. Dinda, S. Kasper, Met. Prog. 109 (1976) 30.